

White dwarf time-series under time-frequency analysis

S. Roques⁽¹⁾, B. Serre⁽¹⁾, N. Dolez⁽¹⁾, K. Bouyoucef⁽¹⁾, P. Marechal⁽²⁾

⁽¹⁾Laboratoire d'Astrophysique de Toulouse, OMP,
14 av. Édouard Belin, F-31400 Toulouse France

⁽²⁾CECM, Simon Fraser university,
Burnaby, B.C. V5A1S6, Canada

RÉSUMÉ

Nous reconstruisons les spectres temporels obtenus à partir de courbes de lumière incomplètes de naines blanches. Le principe de régularisation sous-jacent fait appel à l'interpolation à bande passante limitée et à un processus de poursuite adaptée. Nous illustrons cette étude par un exemple simple, que nous comparons à des données observationnelles WET (Whole Earth Telescope).

ABSTRACT

We reconstruct temporal spectra obtained from incomplete light curves records of white dwarfs. The regularization of the underlying inverse problem makes reference to band-limited interpolation and *matching pursuit*. We illustrate this study with an easy application example and we discuss its degree of confidence by comparing it with WET (Whole Earth Telescope) observations.

1 Astrophysical context

The study of pulsating white dwarfs proves to be an important source of fundamental astrophysical parameters, and may in particular lead to constraints on the theory of stellar evolution [1].

The rich spectrum of their non-radial pulsations may be used to understand how the eigenmodes are driven and damped and then to deduce their global properties (mass, rotation period, magnetic field) and to derive local information on the structure of their outer layers. However, the time scales of these variations are not still well known.

2 Nature of data

In their initial form, the data at our disposal are 10 s integration time light curves (see an example Fig. 1). To take into account the maximum reliable frequency information contained in the observation of a given white dwarf, it is necessary to have as long light curves as possible and in particular to avoid diurnal breaks. Indeed, the case of a one-night observation does not display sufficient resolution to extract directly, from the brightness record of the star information of astrophysical interest.

One way to circumvent this problem is to put a star on a coordinated multi-site observing campaign between telescopes distributed over several longitudes and afterwards to reduce records to individual normalized light curves. In practice, due to weather conditions or other problems, the coverage of the time series that can be obtained remains incomplete (80 %

maximum). Thus, the multi-site transfer function, more than the one-night one, may generate systematic errors.

3 Methodological principles

In all cases (one night or multi-site), the experimental light curves are of the type $\psi(t) = \phi(t)w(t)$ where $w(t)$ is the *observing window function*, so that the dual data (see Fig.1)

$$\widehat{\psi}(u) = \widehat{\phi}(u) \star \widehat{w}(u)$$

in Fourier space are the result of a convolution operation. We are facing a deconvolution problem in Fourier space, and we try to reconstruct the spectrum that would have been obtained with a non-discontinuous or wider observing window function.

Due to the noise and to systematic errors, it is preferable, for a stable reconstruction, to give up restoring the spectrum $\widehat{\phi}(u)$ at its highest level of resolution. One is then led to reconstruct a smoothed version of $\widehat{\phi}(u)$ corresponding to a better but limited time coverage.

The reconstructed spectrum at some level of resolution, is defined as the function minimizing in the mean-squares sense a functional of the type

$$\| g(t)(\widetilde{\psi}(t) - \phi(t)) \|^2$$

where $\widetilde{\psi}(t)$ is obtained from experimental data $\psi(t)$ by some preliminary processing.

The regularization function $g(t)$ to be built depends on the time coverage, on the signal-to-noise ratio and on the target resolution in Fourier space [2].

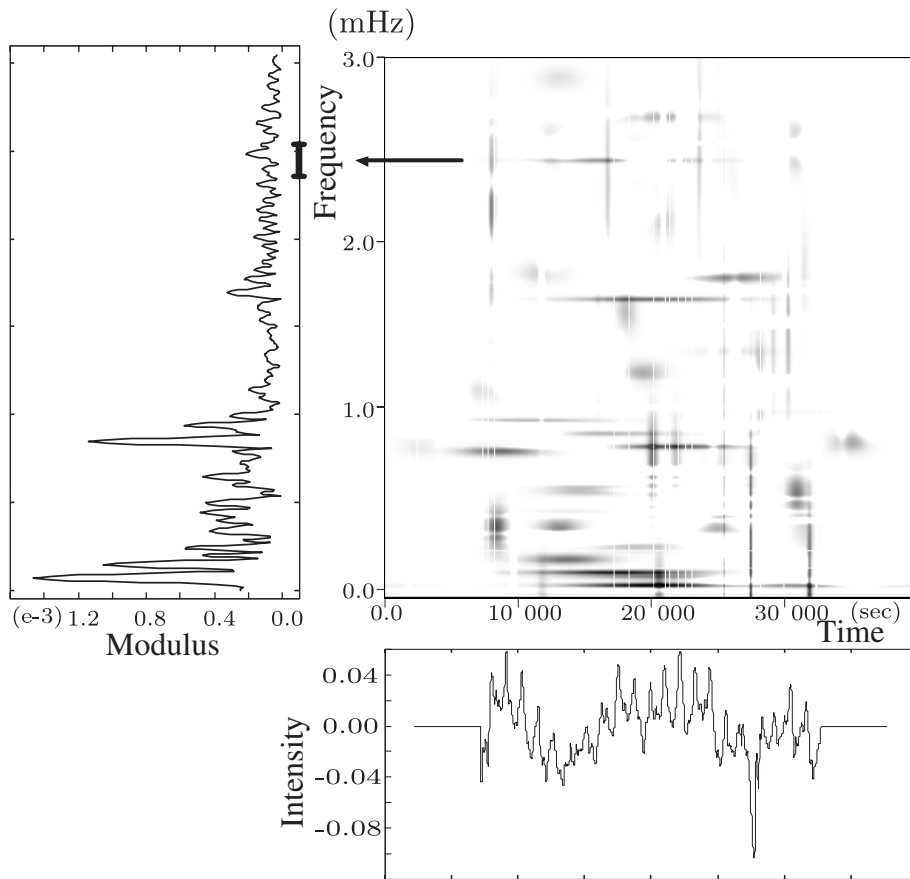


Figure 1 — Time-frequency energy distribution obtained by using the matching pursuit algorithm on the signal presented at the bottom. This signal is the normalized centered light curve of the GD 154, observed on May 17, 1993 at Mauna Kea Observatory. The Fourier transform (in modulus) is recalled on the left. A Gabor dictionary is used, and the algorithm converges after 450 iterations.

4 Regularized inverse problem

The minimum eigenvalue of the “imaging operator” vFg^2F^* conditions the stability of this problem. Here v stands for the characteristic function of the frequency support chosen for deconvolution; F and F^* stand for direct and inverse Fourier transform. This eigenvalue is a function of an *interpolation parameter* characterizing the amount of weighted interpolation to be performed both in real and Fourier spaces. If this eigenvalue happens to be too small, the problem is ill-conditioned and must be reformulated either at a lower level of resolution by changing g , or better by improving the choice of the frequency support v . In this last case, it is judicious to deconvolve over particular ranges of frequencies, but the choice of these intervals turns out to be non-trivial [3].

5 Discrimination of frequency supports

Whereas the choice of a support is easy for low frequencies it is more difficult for high frequencies, because in a noisy part of the spectrum, intervals including low amplitude peaks are hard to select by eye. Moreover, we search oscillations arising almost everywhere in the signal, which are characteristic of

the structural properties of the star. So, it is necessary to get information about the time life corresponding to a given peak in the Fourier spectrum. The particular nature of this problem led us to time-frequency analysis, used as a complement to Fourier analysis, as a way of choosing these supports, and the *matching pursuit algorithm* plays here a decisive role [4].

This speeds up the convergence rate of the deconvolution algorithm and, at the cost of a small edge effect, improves the quality of the solution because the minimum eigenvalue of the imaging operator increases as the support v decreases. As a result, this technique also indicates how to recognize a reconstruction artefact introduced by another deconvolution method, or verifies *a posteriori* whether its results are satisfactory.

6 The matching pursuit algorithm

This algorithm allows us to choose, in a given redundant finite dictionary of time-frequency waveforms, a set of atoms that match the signal as well as possible.

The light curve $\psi(t)$ is approximated with a single vector e^0 of the dictionary:

$$\psi = \langle \psi, e^0 \rangle e^0 + R\psi$$

such that $|\langle \psi, e^0 \rangle|$ is as large as possible.

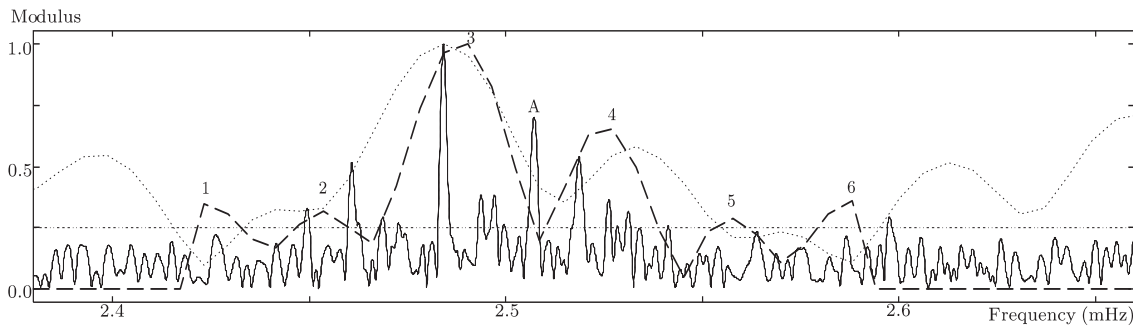


Figure 2 — Full line: raw Fourier data from a multi-site observing campaign. The noisy background is indicated by an horizontal dotted line. Dotted line: raw Fourier data from a one-night observation. Dashed line: result of our deconvolution on the support indicated on Fig. 1.

The main idea of a Matching Pursuit is to sub-decompose the residue $R\psi$, by finding a vector e^1 that matches it as well as possible, as it was done for ψ . And each time, the procedure is repeated on the following residue. It is then possible to build a hierarchy of coherent structures (e^0, e^1, e^2, \dots) yielding a time-frequency energy distribution of the signal.

A frequency support can therefore be defined for each coherent structure extracted presenting sufficiently long time life. The localization of each peak in the Fourier transform can be precisely read on the Y-axis of the matching pursuit diagram. This allows us to detect coherent structures lost in the noise and then to choose a support over which the deconvolution procedure can be set in motion (see the diagram Fig. 1).

7 Deconvolution

Once the deconvolution is performed over one support detected with the Matching Pursuit algorithm, we can set in motion the deconvolution over the following one, and so on. And under the condition that the spectrum of the star can be broken up, we reconstruct it step by step, whereas a global reconstruction was impossible at the same resolution.

As an example of application, we present the deconvolution of a part of the white dwarf DAV GD 154 spectrum, on the support outlined Fig. 1. For a gain in resolution of 2.1, the minimum eigenvalue of the imaging operator is 0.152, and the upper-bound of the relative reconstruction error is 15 per cent. In 13 iterations, the method of conjugate gradients provides the least-squares solution presented in Fig. 2. It is not surprising to observe additional information, and in particular the splitting of the two main peaks. The raw data of a multi-site observing campaign are also represented on this figure. One can note that in such multi-site data there is a strong noisy background essentially due to the side lobes of the impulse response.

We can verify that the information contained in peaks (1) to (6) of our deconvolution is also contained at higher resolution. For example, peak (3) includes in fact three peaks and this is why its maximum appears centered over these three peaks. The same effect is present for peak (2). Note that peak (A) is an

artifact, resulting from a systematic error due to the segmented nature of the multi-site observing window.

Bibliography

- [1] D. Koester and G. Chanmugam, “Physics of white dwarfs stars”, Reports on Progress in Physics, 53, pp. 837-915, 1990.
- [2] A. Lannes, S. Roques and M.J. Casanove, “Resolution and robustness in image processing: a new regularization principle”, J. Opt. Soc. Am. A, Vol. 4, No. 1, pp. 189-99, 1987.
- [3] S. Roques, B. Serre and N. Dolez, “Band limited interpolation of multiperiodic white dwarf time-series”, submitted to MNRAS.
- [4] S. Mallat and Z. Zhang, “Matching pursuit with time-frequency dictionaries”, IEEE Trans. Signal Process., 41(12), pp. 3397-3415, 1993.